Macromolecular Bioscience
www.mbs-journal.de

A Ninhydrin-Type Urea Sorbent for the Development of a Wearable Artificial Kidney

*Jacobus A. W. Jong, Yong Guo, Diënty Hazenbrink, Stefania Douka, Dennis Verdijk, Johan van der Zwan, Klaartje Houben, Marc Baldus, Karina C. Scheiner, Remco Dalebout, Marianne C. Verhaar, Robert Smakman, Wim E. Hennink, Karin G.F. Gerritsen, and Cornelus F. van Nostrum**

The aim of this study is to develop polymeric chemisorbents with a high density of ninhydrin groups, able to covalently bind urea under physiological conditions and thus potentially suitable for use in a wearable artificial kidney. Macroporous beads are prepared by suspension polymerization of 5-vinyl-1-indanone (vinylindanone) using a 90:10 (v/v) mixture of toluene and nitrobenzene as a porogen. The indanone groups are subsequently oxidized in a one-step procedure into ninhydrin groups. Their urea absorption kinetics are evaluated under both static and dynamic conditions at 37 °C in simulated dialysate (urea in phosphate buffered saline). Under static conditions and at a 1:1 molar ratio of ninhydrin: urea the sorbent beads remove ≈0.6–0.7 mmol g^{-1} and under dynamic conditions and at a 2:1 molar excess of ninhydrin ≈0.6 mmol urea g^{-1} sorbent in 8 h at 37 °C, which is a step toward a wearable artificial kidney.

1. Introduction

Waste compounds such as urea, creatinine, potassium, phosphate, and excess water accumulates in the body of patients suffering from end-stage kidney disease. These patients undergo dialysis sessions in the hospital or dialysis centers during which these waste solutes diffuse over a nanoporous membrane, effectively removing these waste solutes from their body.[1] To improve the quality of life of dialysis patients, wearable artificial kidney devices are being developed which use a small volume of dialysate (preferably <0.5 L) that is continuously regenerated by a purification unit and re-used in a closed loop system.[2–4] Removal of urea from dialysate is a major challenge in the realization of such a wearable dialysis device,[5,6] since urea has low reactivity and high aqueous solubility while it is the metabolite with the highest daily molar production (240–470 mmol day^{-1}).[7,8] It has been estimated that a urea clearance of 25–49 mL min^{-1} is needed in a 8-h dialysis session to keep the urea concentration below 20 mM.[6] Several strategies for urea removal from dialysate have been explored,[6] including enzymatic hydrolysis,[9,10] electro-oxidation,[11] and adsorption of urea.[12–16] However, each of these strategies has drawbacks that do not allow reduction of the dialysate volume to <0.5 L as required for a wearable device.[6,17]

Chemisorption of urea by a sorbent, that is able to form irreversible covalent bonds with urea at 37 °C, seems an attractive strategy as 1) high urea binding capacities (BC) have been reported[13,18–20] and 2) no potentially harmful side products are formed. Several urea chemisorbents have been reported in

Dr. J. A. W. Jong, Dr. Y. Guo, S. Douka, K. C. Scheiner, Dr. W. E. Hennink, Dr. C. F. van Nostrum
Department of Pharmaceutics
Utrecht Institute for Pharmaceutical Sciences (UIPS)
Utrecht University
Universiteitsweg 99 3584 CG, Utrecht, the Netherlands
E-mail: C.F.vanNostrum@uu.nl

Dr. J. A.W. Jong, D. Hazenbrink, Dr. M. C. Verhaar, Dr. K. G. F. Gerritsen
Department of Nephrology and Hypertension
University Medical Centre Utrecht
3584 CX, Utrecht, the Netherlands

The ORCID identification number(s) for the author(s) of this article can be found under https://doi.org/10.1002/mabi.201900396.

DOI: 10.1002/mabi.201900396

D. Verdijk
MercaChem B.V.
Kerkenbos 1013, 6546 BB, Nijmegen, the Netherlands

J. van der Zwan, Dr. K. Houben, Dr. M. Baldus
NMR Spectroscopy, Bijvoet Center for Biomolecular Research
Utrecht University
Padualaan 8, 3584 CH Utrecht, the Netherlands

R. Dalebout
Inorganic Chemistry and Catalysis
Debye Institute for Nanomaterials Science
Utrecht University
Universiteitsweg 99, 3584 CG, Utrecht, the Netherlands

Dr. R. Smakman
Innovista
Raadhuisstraat 1 1393 NW, Nigtevecht, the Netherlands

literature; however, the main drawbacks are that the kinetics of urea adsorption are generally very slow and that these sorbents need multi step synthesis, which routes are difficult and expensive to scale up.[13–14,19,21]

Our aim is to develop urea sorbents with fast urea removal kinetics which are relatively easy to synthesize. Recently, we reported the second-order reaction rate constants (k_2-values) of more than 30 carbonyl compounds with urea in buffered aqueous solution, of which ninhydrin was one of the compounds with the fastest binding kinetics.[22]The reaction of 5-substituted-ninhydrin with urea is shown in **Scheme 1A**. In addition, we investigated the effect of electron donating and electron withdrawing substituents on the reactivity of ninhydrin toward urea, and found that an electron donating group such as a methyl- or a tert-butyl- group on the 5-position shows the highest reactivity of the ninhydrin derivates with urea.[23] Therefore, we concluded that a sorbent with an electron-donating carbon–carbon backbone, functionalized with ninhydrin groups on the 5-position would structure-wise be optimal.

Smakman and van Doorn previously developed macroporous urea sorbents containing accessible ninhydrin-groups.[19,24] These sorbents were obtained by suspension copolymerization of styrene with divinylbenzene (DVB), followed by a six-step modification which resulted in sorbent particles of which 55% of the styrene groups were modified into ninhydrin groups (supporting information section 1).[19,24] The intermediate obtained after five modification steps is one in which the aromatic groups of polystyrene were modified into 1-indanone groups, which were subsequently oxidized to ninhydrin groups in a one-pot halogenation and Kornblum oxidation reaction (scheme 1B).[19] The resulting sorbents are among the best performing in terms of binding capacity so far (2.2 mmol g^{-1}).[18,24]

We hypothesized that the density of ninhydrin groups in such a sorbent could be increased by directly polymerizing a 1-indanone-based monomer followed by a single final oxidation step, thereby avoiding the first five post-polymerization modification steps which yielded incomplete conversion of the aromatic groups into ninhydrin groups. Therefore, we selected 5-vinyl-1-indanone[25] (vinylindanone) as the monomer instead of styrene, because this results in a 5-alkyl-substituted ninhydrin group after oxidation, which, as discussed above, has structure-wise optimal reactivity toward urea (Scheme 1C).

Further, microparticles with a size of 100–1000 μm are preferred for application in a sorbent cartridge to prevent pressure building up in the dialysate circuit.[26] In addition, we assumed that a macroporous system would be required to increase the accessibility of the ninhydrin groups in the beads for urea and to obtain fast binding kinetics.[13]

The aim of this study is therefore to design, prepare, and characterize macroporous sorbent beads with a high density of ninhydrin groups obtained by suspension polymerization of vinylindanone, followed by a one-step oxidation of the indanone groups into ninhydrin groups. The urea binding of the obtained beads was studied under both static and dynamic (flow) conditions from simulated dialysate (urea in PBS), aiming for the application of regeneration of dialysate in a wearable dialysis device.

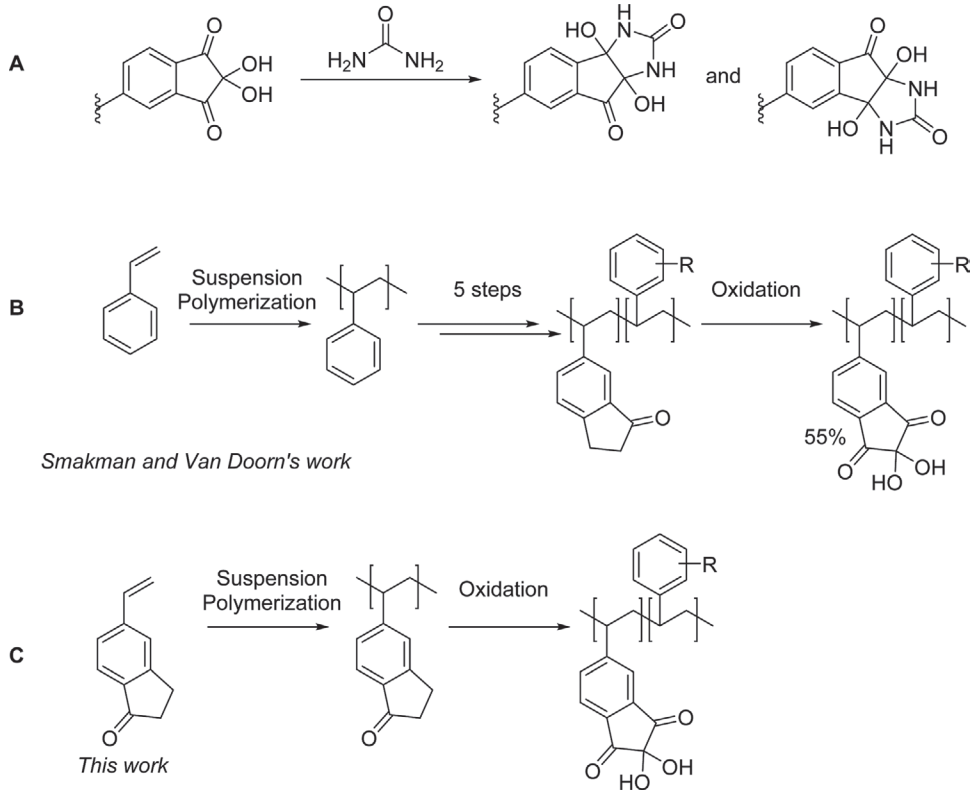

Scheme 1. A) The reaction of 5-substituted ninhydrin with urea[23] and B) synthesis of ninhydrin sorbents via Smakman's route[19,24] and C) the route described in this work. R = side products.

2. Results and Discussion

2.1. 5-Vinyl-1-Indanone Synthesis and Upscaling

The functional monomer 5-vinyl-1-indanone (vinylindanone) was synthesized on a relatively small scale of 4 g in three steps from 5-bromoindan-1-one (Scheme S2, Supporting Information). The first and the second step, a Sonogashira cross-coupling of 5-bromo-1-indanone with ethynyltrimethylsilane followed by deprotection of the TMS-group, was reported by Ortega et al. yielding 5-ethynylindan-1-one.[27] In the third step, the alkyne was reduced to a vinyl-group using H_2 and Lindlar's catalyst. The overall yield over these three steps (of which two steps included purification by column chromatography) was 73%.

Although this route is suitable to obtain vinylindanone on a small scale (up to 40 g), the purification by column chromatography (needed for two steps) proved to be cumbersome on a larger scale. Therefore, in order to obtain vinylindanone on 500 g scale, a one-step synthesis by a Suzuki-Molander coupling of 5-bromo-1-indanone with potassium vinyltrifluoroborate was exploited (Scheme S3, Supporting Information).[28] The reaction conditions were optimized until almost quantitative conversion (Section S2, Supporting Information) and vinylindanone was isolated after filtration over a silica plug in a 85% yield. Vinylindanone obtained via the Suzuki–Molander route yielded a monomer with higher purity than vinylindanone synthesized on a small scale, as both the melting point and the melting enthalpy were substantially higher (26 and 42 °C; 22.9 and 92.8 J mol^{-1}, respectively).

2.2. Polyvinylindanone Synthesis and Optimization

Macroporous polyvinylindanone (pVI) particles can be obtained by suspension polymerization of vinylindanone and divinylbenzene (DVB) using a non-solvating porogen, which is able to dissolve the used monomers (vinylindanone and DVB), and on the other hand precipitates the resulting polymer (**Figure 1**). This in turn causes phase separation between the monomer solution and the precipitated polymer yielding porous structures.[29] A commonly used method to predict the miscibility of solvents, monomers, and polymers, is comparing the Hildebrand solubility parameters (δ) as similar δ values indicate miscibility. This solubility parameter, which is defined as the square root of the cohesive energy density, can either be determined experimentally or calculated based on the molecular structure via various methods.[30,31] For the preparation of porous particles using a non-solvent, a porogen is needed with a δ-value close to that of the monomer to ensure its dissolution, and different (preferable lower) than that of the resulting polymer, resulting in its precipitation. The δ-values of vinylindanone and poly-vinylindanone (pVI), as calculated based on the method reported by Fedors,[31] are much larger that the δ-values of styrene and polystyrene (20.5 and 22.9 vs 17.8 and 17.4–19.0 $J^{1/2}m^{-3/2}$, respectively see supporting information section 3[30,32]). The porogen mixture used for the preparation of porous polystyrene particles has a delta-value (δ_{mix}) of 15.2 $J^{1/2}m^{-3/2}$, which is lower than the δ-values of both styrene and polystyrene (lower by 2.6 and 2.2–3.8 $J^{1/2}m^{-3/2}$, respectively). Therefore, a porogen is needed with a larger δ-value than the one used for the suspension polymerization of polystyrene. Vinylindanone is soluble in both toluene (δ = 18.2 $J^{1/2}m^{-3/2}$)[30,33] and nitrobenzene (δ = 21.7 $J^{1/2}m^{-3/2}$)[34] whereas pVI is insoluble in toluene but soluble in nitrobenzene. The δ-value of a mixture (δ_{mix}) is calculated with Equation ((1)), in which x_i, V_i, and δ_i are the molar fraction, the volume fraction, and the (calculated) δ-values of the solvents and monomer, respectively.

$$\delta_{mix} = \frac{\Sigma x_i V_i \delta_i}{\Sigma x_i V_i} \quad (1)$$

Using mixtures of nitrobenzene and toluene as non-solvating porogen, the conditions (i.e., toluene: nitrobenzene ratio) to obtain macroporous pVI beads prepared by suspension copolymerization of vinylindanone and DVB were systematically optimized. First, the volume fraction of nitrobenzene used in the porogen mixture was increased with steps of 5%, and the S_{BET} surface areas of the obtained beads were measured with N_2 physisorption (Figure 1). The highest S_{BET} surface area of 1.7 m^2 g^{-1} was obtained using a mixture of 90% toluene and 10% nitrobenzene as porogen (δ_{mix} = 18.9 $J^{1/2}m^{-3/2}$ with ≈43% v/v vinylindanone and 18.2 $J^{1/2}m^{-3/2}$ without vinylindanone), which indeed has a lower δ_{mix}-value than the calculated δ-value of the monomer (20.4 $J^{1/2}m^{-3/2}$). Therefore this mixture was identified as the optimal porogen for the preparation of macroporous pVI beads via suspension polymerization.

With the optimized porogen composition established for the suspension polymerization of vinylindanone at hand, the synthesis of the beads was scaled up to 24 and 50 g yielding beads with a S_{BET} of 1.5 and 3.3 m^2/g in 80 and 92% yield, respectively.

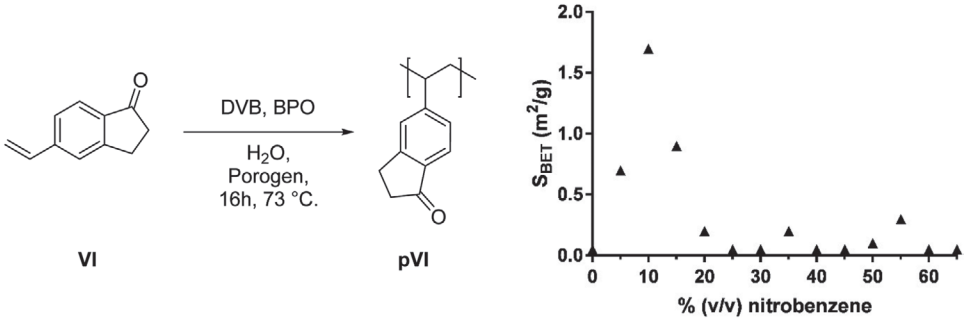

Figure 1. Reaction scheme of the suspension polymerization of 5-vinylindan-1-one (vinylindanone), and plot of the S_{BET} surface area of the obtained pVI (with 2.5% DVB) beads versus the volume fraction (% v/v) nitrobenzene in toluene used as porogen in the suspension polymerization.

2.3. Oxidation of Polyvinylindanone

The oxidation of indanone groups present in the macroporous sorbent particles into ninhydrin groups was studied by a one-step halogenation and Kornblum oxidation reaction using HBr, HI, and I_2 in DMSO at 90 °C (**Figure 2**). Beads were removed from the suspension at different time points and their urea binding capacity was determined. Figure 2 shows that indanone groups in pVI were gradually oxidized into ninhydrin groups to reach a BC for urea of 2.8 mmol g^{-1} in 24 h. The observation that the BC reaches a plateau value demonstrates that the formed ninhydrin groups are stable under these harsh oxidizing conditions. Next, pVI beads were oxidized on a 40-g scale under these conditions for 24 h, yielding 49.1 g sorbent beads containing ninhydrin groups (pVI-Ox). The BC of the obtained pVI-Ox beads was 3.2 mmol g^{-1}, which is one of the highest reported urea binding capacities of sorbents reported so far.[18,35,36]

2.4. Characterization of pVI and pVI-Ox

Photographs of pVI and pVI-Ox beads are shown in **Figure 3**A,D, respectively, and their morphologies were analyzed with scanning electron microscopy (SEM, Figure 3B,C,E,F). The images of Figure 3 show typical examples of both pVI and pVI-Ox beads, which are present as single beads (B and E) and as aggregates of several beads (C and F). The diameters of the pVI and pVI-Ox (aggregated) beads as determined by light microscopy were 0.74 ± 0.31 and 0.73 ± 0.28 mm, respectively. The surface area of pVI-Ox beads as determined by N_2 physisorption was 1.7 m^2 g^{-1}, demonstrating that the porosity was not affected during the oxidation of the indanone groups (S_{BET} = 1.5 m^2 g^{-1}). Thermal analysis by differential scanning calorimetry (DSC) showed that the glass transition temperature of both polymers was >160 °C (Section S5, Supporting Information) explaining their dimensional stability under the oxidizing conditions.

The pVI and pVI-Ox beads were analyzed by infrared (IR) spectroscopy, and their spectra were compared with those of commercial 1-indanone and ninhydrin (supporting information section 4). The stretching vibration of the C=O bond (1700 cm^{-1}) and of the aromatic C=C bonds (1600 cm^{-1}) in the spectrum of pVI correspond to their respective peaks in the spectrum of 1-indanone. Similarly, the stretching vibrations of the C=O bonds (1700 and 1750 cm^{-1}), the aromatic C=C bonds (1600 cm^{-1}) and the C—O bonds (1090 cm^{-1}) in the IR spectrum of pVI-Ox are very similar to those of ninhydrin. In addition, the C—O stretching vibration peak (1090 cm^{-1}) as well as the splitting of the C=O peak observed (1780–1700 cm^{-1}) in the IR spectrum of pVI-Ox are not present in that of pVI, thereby confirming that the indanone groups have indeed been converted into ninhydrin groups during the oxidation step.

Because IR analysis does not provide information on the extent of oxidation of the indanone groups, both pVI and pVI-Ox were analyzed with ^{13}C-solid state NMR spectroscopy. The different carbon signals present in the spectrum of the beads were intensified using cross-polarization (CP),[37] which, however, does not allow quantitative integration of the peaks (**Figure 4A**). In the CP-spectrum of pVI (upper spectrum) a sharp peak at 30 ppm is observed, corresponding to the CH_2 groups of the indanone moiety. In the CP spectrum of pVI-Ox (lower spectrum) this sharp peak has disappeared, which demonstrates that the indanone groups were fully converted. In addition, a new peak around 90 ppm was detected, which is assigned to the hydrate carbon of ninhydrin. In order to quantify the density of ninhydrin groups present in pVI-Ox, the recycle delay (time in between the pulses) has to be increased to allow all carbons to reach the equilibrium position. Therefore, the relaxation time (T_1) of pVI-Ox was determined to be 40 s and a quantitative solid state ^{13}C- NMR spectrum was obtained using a recycle delay of 80 s ($2*T_1$), applying a 30° pulse. The quantitative ^{13}C- solid state NMR spectrum is shown in Figure 4B. Integration of the C—C backbone peak (30–50 ppm) and the hydrate carbon peak (90 ppm) demonstrates that 74% of the indanone groups were converted into ninhydrin groups. The structure of the remaining ≈24% of the converted indanone groups could not be established as these side products did not give rise to new peaks in the ^{13}C-NMR spectrum (Figure 4A,B). Based on the molecular weight of vinyl-substituted ninhydrin (204 g $mmol^{-1}$), the maximum binding capacity that could be obtained using sorbent beads consisting of 97.5% vinylninhydrin and 2.5% DVB is 4.8 mmol g^{-1}. A binding capacity of pVI-Ox of 3.2 mmol g^{-1} implies that 67% (3.2/4.8 mmol g^{-1} *100%) of

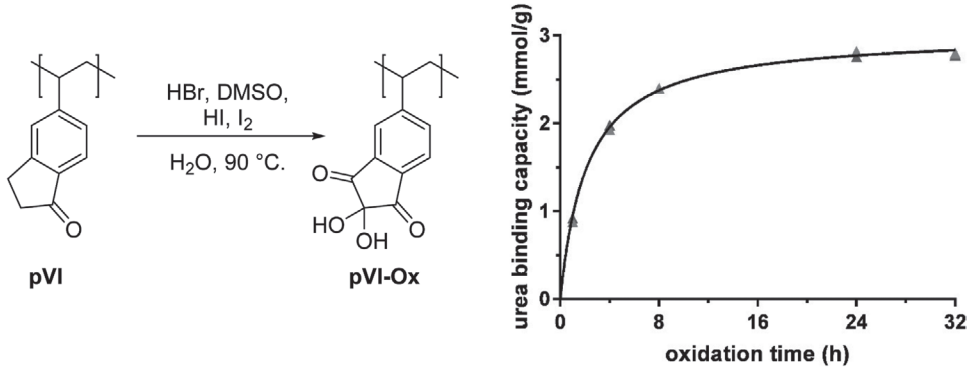

Figure 2. Reaction scheme of the oxidation of indanone groups in pVI into ninhydrin groups (pVI-Ox), and plot of the urea binding capacity (average of two independent experiments, red and blue) of sorbent beads as function of oxidation time of pVI.

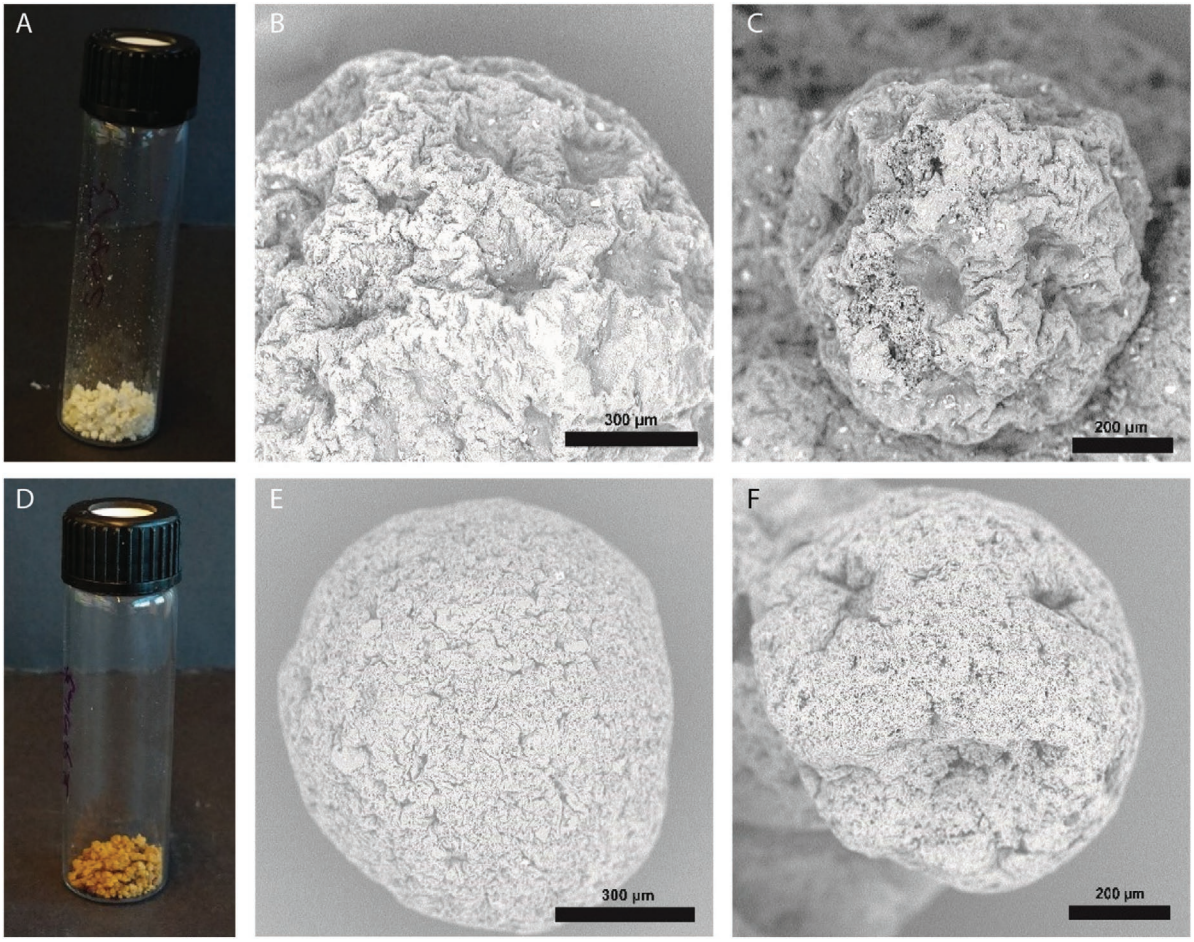

Figure 3. A,D) Photographs and B,C, E, F) SEM picturesof pVI and pVI-Ox beads.

the indanone groups are converted into accessible ninhydrin groups. Considering the error in both the urea binding capacity and the quantitative solid state ^{13}C-NMR analysis (≈5%) as well as the likely presence of residual water in the beads, it is concluded that all ninhydrin groups present in pVI-Ox are accessible for urea.

2.5. Kinetics of Static Urea Absorption by pVI-Ox Beads

To establish the potential of pVI-Ox beads as a suitable urea sorbent for dialysate regeneration, their urea removal kinetics were evaluated. First, to assess the urea absorption kinetics of pVI-Ox beads and the influence of temperature under static conditions, the beads were incubated with a 30 mM urea solution in PBS at 37, 50, and 70 °C and the urea concentration in the supernatant was monitored for 24 h (**Figure 5A**).

At 37 and 50 °C the rate of the urea binding is relatively slow and therefore the amount of urea bound is almost linear with time during the first 8 h, as the amount of available ninhydrin groups is still large (≥78% (2.5 mmol g^{-1}) at 37 °C and ≥69% (2.2 mmol g^{-1}) at 50 °C). At 70 °C, however, the urea binding kinetics is much faster, and the binding kinetics decrease quickly after 6–8 h because both the amount of available ninhydrin groups and the urea concentration have decreased by >50%.

The second-order rate constant (k_2) of the reaction of urea with the ninhydrin-groups at 37 °C, as determined from the slope of the plot of the inverse urea concentration in time (supporting information section 8),[23] was determined to be 1.1 ± 0.1 $M^{-1}h^{-1}$. This is close to our earlier reported k_2-value of the reaction of urea with ninhydrin at 37 °C (2.7±0.1 $M^{-1}h^{-1}$)[22] and our earlier observation that alkyl substituents decrease the reactivity of ninhydrin-derivatives toward urea with factor ≈2.[23] The natural logarithm of the k_2-values was plotted versus the inverse absolute temperature (Figure 5B). From this Arrhenius plot the activation energy (E_a) and pre-exponential factor (A) for the reaction of urea with the ninhydrin-groups in pVI-Ox were determined to be 10.8 ± 0.5 kcal mol^{-1} and (48.4 ± 2.1) × 10^6 $M^{-1}h^{-1}$. Interestingly, the activation energy of this reaction is lower than that of the reaction of ninhydrin with urea in solution (14.0 ± 0.4 kcal mol^{-1}), and the pre-exponential factor, which is correlated to the number of collisions between the reactants, is greatly reduced with a factor ≈10^3 ((23.2 ± 0.6) × 10^9 $M^{-1}h^{-1}$),[22] likely due to the strongly reduced mobility of the ninhydrin groups in the beads as compared to ninhydrin in

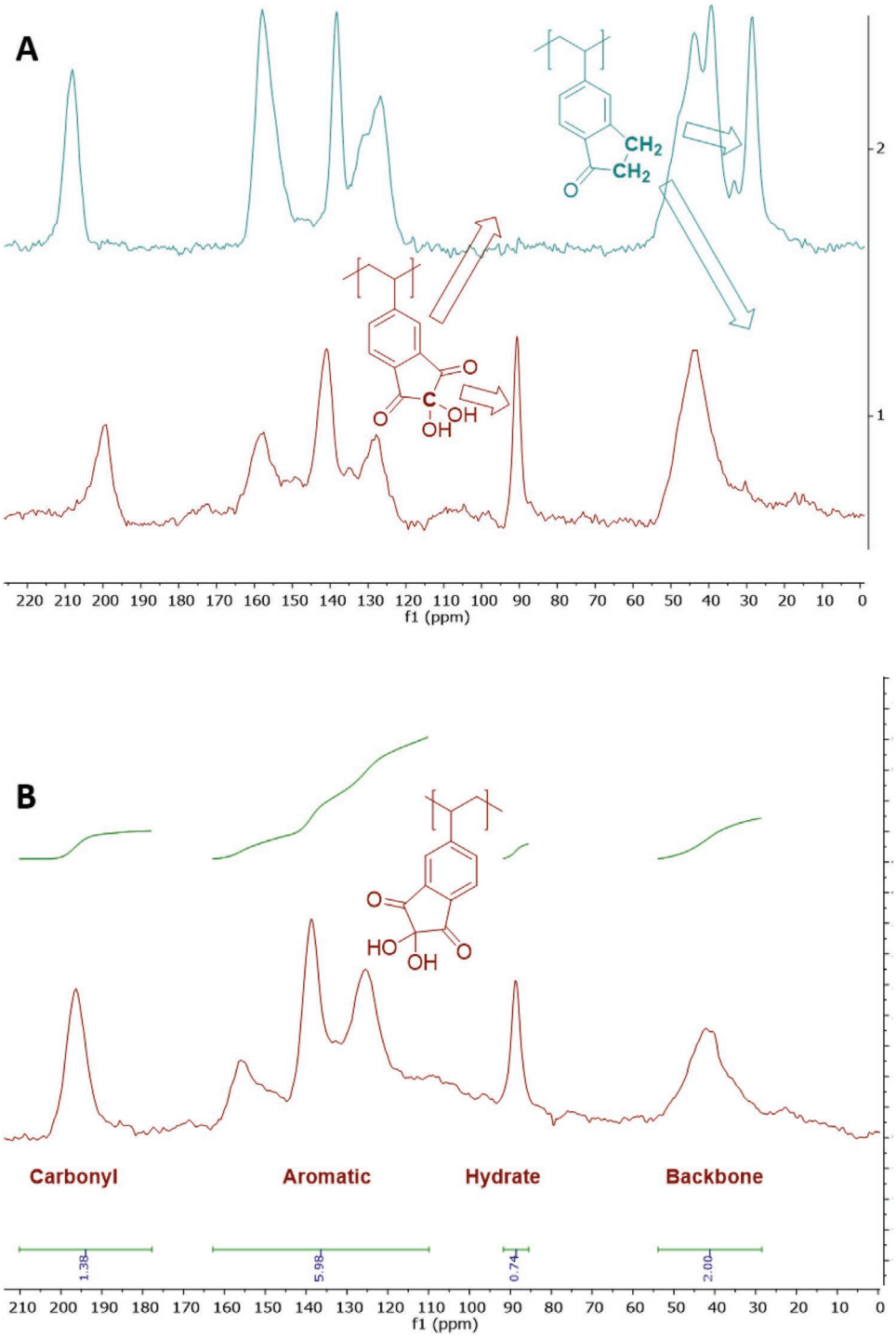

Figure 4. A) Solid state ^{13}C NMR (CP) spectra of pVI (upper) and pVI-Ox (lower). B) Quantitative solid state ^{13}C-NMR (30° pulse and recycle delay = $2*T_1$) of pVI-Ox. Integration of the hydrate carbon (90 ppm) and the backbone (30–50 ppm) shows that 74% of the indanone groups were converted into ninhydrin groups.

solution. Apparently, it is a coincidence that the k_2-value of the reaction of the ninhydrin groups in the sorbent with urea at 37 °C is similar to that of ninhydrin with urea in solution as the decrease in the pre-exponential factor (A) is compensated by a decrease in activation energy (E_A).

2.6. Effect of Ninhydrin: Urea Molar Ratio on the Urea Removal

To study the effect of the molar ratio between urea in solution and the ninhydrin groups in pVI-Ox on urea removal, the amount of sorbent was doubled as compared to the conditions

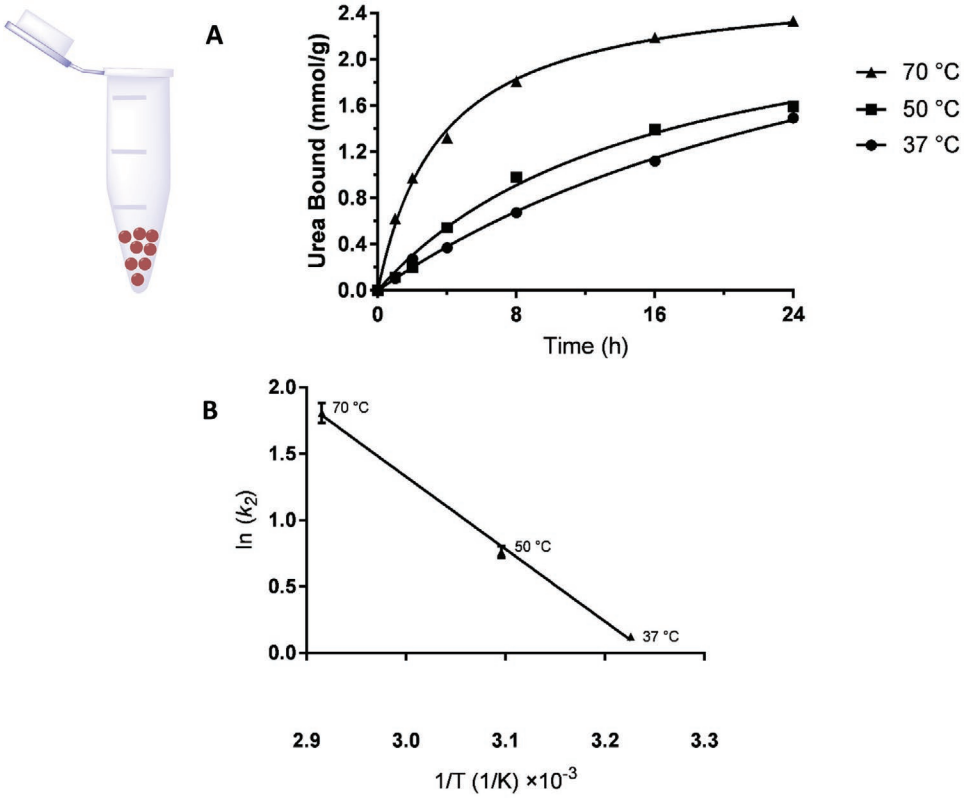

Figure 5. A) Binding of urea by pVI-Ox beads in time under static conditions at 37, 50, and 70 °C. B) Arrhenius plot of the reaction of urea with ninhydrin-groups in pVI-Ox. Glass vials were charged with pVI-Ox beads (50 mg, 0.16 mmol ninhydrin groups), suspended in a 30 mM urea solution in PBS (5 mL, 0.15 mmol urea) and incubated in an oven under constant rotation and at the indicated temperatures. At regular time points the urea concentrations in the supernatants were measured. Each data point in Figure 5A is the average of two independent measurements.

in Figure 5. **Figure 6A** shows that, as expected, the urea concentration dropped more rapidly at a higher molar ratio of ninhydrin: urea. The determined k_2 value for the reaction of ninhydrin and urea at a 1:1 molar ratio and at 37 °C was (1.1 ± 0.1 $M^{-1}h^{-1}$, Figure S8 and Table S9, Supporting Information). To determine the k_2-value for the reaction of ninhydrin groups with urea in a 2:1 molar ratio, pseudo-first order conditions are assumed for the first 4 h. The pseudo-first order rate constant (k_{PFO}) was determined to be 0.060 h^{-1}, which corresponds a k_2-value of 1.0 ± 0.1 $M^{-1}h^{-1}$ (Figure S9, Supporting Information) and is in good agreement with the value determined at a 1:1 molar ratio. The data of Figure 6A were used to calculate the amount of urea bound per gram of sorbent. Figure 6B shows that the pVI-Ox beads bound ≈0.5 and ≈0.6 mmol urea g^{-1} in 8 h when the molar ratio ninhydrin: urea were 2:1 and 1:1, respectively.

2.7. Urea Binding of Urea on pVI-Ox Beads under Dynamic Conditions

To simulate the conditions of a dialysis session better than with static sorption, pVI-Ox beads were packed in a glass column and 30 mM urea in PBS, a concentration representative for dialysate,[38] was continuously pumped from a 37 °C reservoir in an Erlenmeyer through the sorbent column back into the Erlenmeyer (**Figure 7A**). To compare with the binding under static conditions (Figure 6B), the ninhydrin: urea molar ratio was 2:1. Figure 7B shows that the amount of urea that is bound (in mmol g^{-1}) under dynamic flow conditions was 0.6 mmol g^{-1} in 8 h.

The total amount of urea removed from solution was $4 \times 0.6 = 2.4$ mmol in 8 h, thus 0.3 mmol h^{-1}. Therefore the clearance (i.e., the volume completely cleared of urea) was 10 mL h^{-1}. This clearance is relatively low as only 4 g of sorbent was used, and it is expected that the clearance can be increased to clinically relevant values (25–49 mL min^{-1}[6]) by increasing the amount of sorbent. **Figure 8** shows the urea removal by pVI-Ox both under static conditions (from Figure 6B) and dynamic conditions (from Figure 7B) with the ninhydrin groups in the sorbent and urea in solution in a 2:1 molar ratio. The sorbent showed similar urea binding characteristics under static and dynamic conditions, especially during the first 4 h. This can be explained by the fact that the flow rate (25 mL min^{-1} thus 1500 mL h^{-1}) was much higher than the clearance (10 mL h^{-1}) and thus did not limit the urea removal. Future studies aim to translate the kinetics of urea removal by pVI-Ox at the small scale to a clinically relevant system for the regeneration of dialysate, by employing appropriate flow rates and amounts of sorbent.

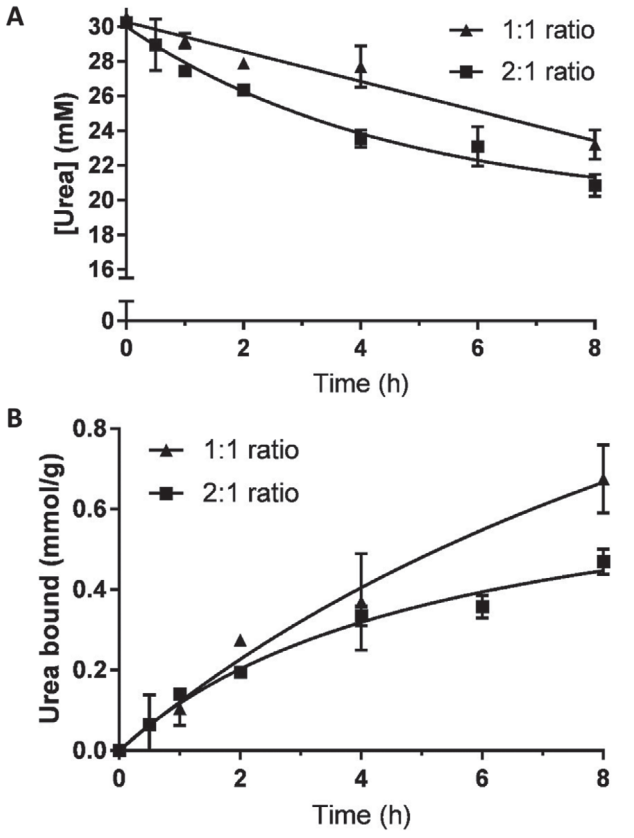

Figure 6. Urea removal of pVI-Ox beads at 37 °C at different ninhydrin: urea molar ratios. A) Plot of the urea concentration in time. B) Plot of the amount of urea bound per gram of sorbent in time.

3. Conclusions

This study reports an easy and scalable method to obtain a sorbent with high density of ninhydrin groups for urea removal from dialysate, which is crucial for realization of a wearable artificial kidney. The sorbent was obtained by suspension polymerization of 5-vinyl-1-indanone, followed by a single oxidation step, yielding a sorbent of which the backbone is 74% functionalized with ninhydrin groups (based on quantitative solid state ^{13}C-NMR). The beads have a maximum urea binding capacity of 3.2 mmol g^{-1} indicating that all ninhydrin groups are accessible for urea.

It was found that the second order constant at 37 °C of the reaction of urea and ninhydrin groups of the beads was equal to that of the reaction in solution, with a reduced number of collisions compensated by a lower activation energy.

Static and dynamic binding studies suggest that ≈600 grams of pVI-Ox beads are sufficient to remove the daily urea production of a patient (≈400 mmol) within an 8-h dialysis session, which brings the development of a wearable kidney a step closer to reality.

4. Experimental Section

Chemicals and Materials: All materials were obtained from Sigma-Aldrich (Zwijndrecht, the Netherlands) and used as received unless stated otherwise. 5-Bromoindaone was obtained from CombiBlocks (San Diego, CA). Phosphate buffered saline (PBS, pH = 7.4, ion composition: Na^+ 163.9 mM, Cl^- 140.3 mM, HPO_4^{2-} 8.7 mM, $H_2PO_4^-$ 1.8 mM) was obtained from B. Braun (Melsungen AG, Germany). Anhydrous dicalcium phosphate ($CaHPO_4$) was obtained from Chemtrade International (Bussum, the Netherlands). Polymethacrylic acid (Degalan RG S mv) was obtained from Evonik Industries (Darmstadt, Germany). Flash chromatography was performed over silica gel (particle size 40–63 µm, VWR Chemicals, Leuven, Belgium) using the indicated eluent.

NMR and IR Spectroscopy and TLC: ^{1}H- and ^{13}C- liquid NMR spectra were recorded using an Agilent 400-MR DD2 equipped with a OneNMR probe at RT. Residual solvent signals were used as internal standard (^{1}H: δ 7.26 ppm, ^{13}C (^{1}H): δ 77.16 ppm for $CDCl_3$). Chemical shifts (δ) are given in ppm and coupling constants (J) are given in hertz (Hz). Resonances are described as s (singlet), d (doublet), t (triplet), q (quartet), bs (broad singlet), and m (multiplet) or combinations thereof. Infrared (IR) spectra were recorded neat using a Perkin Elkmer ATRU Spectrum 2 and reported in cm^{-1}. Thin Layer Chromatography (TLC) was performed using plates from Merck Darmstadt, Germany, (SiO_2,

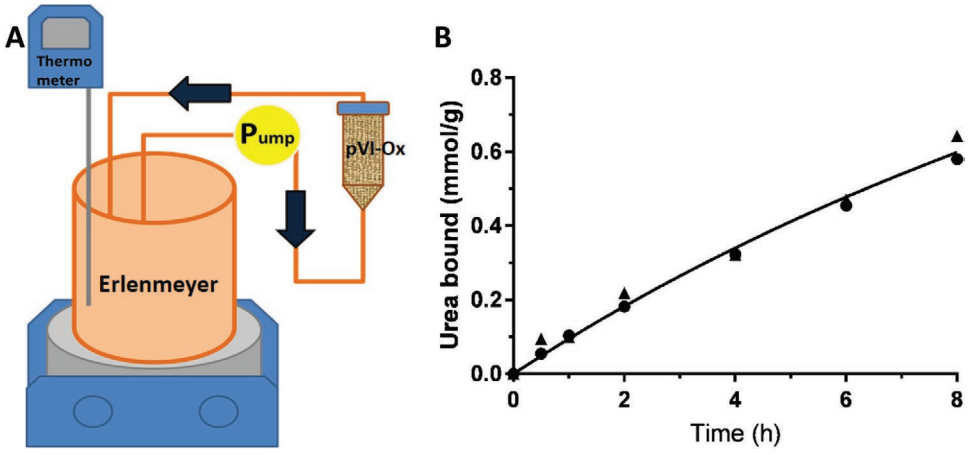

Figure 7. Binding of urea by pVI-Ox beads in time under dynamic conditions at 37 °C. A) Schematic representation of the experimental set up. B) Plot of the urea bound in time. The line shows a fit of the average amount of urea bound in time. Conditions: total volume 200 mL, 4.0 g pVI and a flow rate of 25 mL min^{-1} (N = 2).

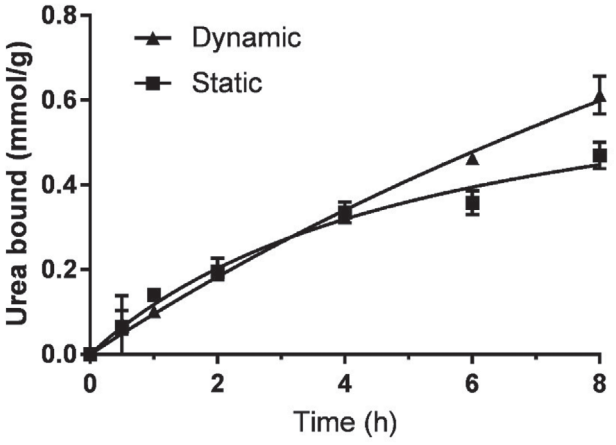

Figure 8. Urea bound by pVI-Ox from a 30 mM urea solution in time under static and dynamic conditions at 37 °C. Molar ratio ninhydrin: urea is 2:1.

Kieselgel 60 F254 neutral, on aluminum with fluorescence indicator) and the compounds were visualized by UV detection (254 nm).

Determination of Solute Concentrations: Urea concentrations were determined with an AU 5800 routine chemistry analyzer (Beckman Coulter, Brea, CA) using a coupled enzyme reaction,[39] which results in a colorimetric (570 nm) product proportional to the urea concentration.

Synthesis of 5-Vinyl-1-Indanone (3-Step Route): Synthesis of 2,3-dihydro-5-[2-(trimethylsilyl)ethynyl]inden-1-one.[27]

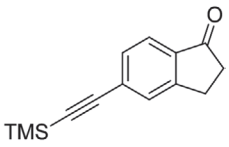

In a flame-dried three-neck round bottom flask under nitrogen atmosphere, to a mixture of 5-bromo-1-indanone (44.3 g, 210 mmol, 1.0 eq.), $(Ph_3P)_2PdCl_2$ (1.4 g, 1 mol%,) and CuI (799 mg, 2 mol%) in 3:1 anhydrous Et_3N:DMF (350 mL) trimethylsilylacetylene (43.6 mL, 315 mmol, 1.5 eq.) was added slowly. The reaction mixture was then heated to 80 °C for 2 h and monitored by TLC until full conversion was observed. The reaction mixture was allowed to cool to room temperature (RT) and was transferred into a separation funnel. The mixture was extracted with CH_2Cl_2 and which phase was subsequently washed with water. The organic layer was further washed with 10% HCl, 10% Na_2CO_3, and water and then dried over Na_2SO_4, filtrated, and concentrated. The residue was purified by flash chromatography on silica gel (4:1 EtOAc:hexane gradient to 1:1 EtOAc:hexane), and 2,3-dihydro-5-[2-(trimethylsilyl) ethynyl]inden-1-one was isolated as a solid (40.5 g, 84%). ^{1}H NMR (400 MHz, $CDCl_3$) δ 7.68 (*d*, J = 7.9 Hz, 1H), 7.57 (*s*, 1H), 7.44 (*d*, J = 7.9 Hz, 1H), 3.11 (*t*, J = 5.9 Hz, 2H), 2.71–2.68 (*m*, 2H), 0.26 (*s*, 9H). ^{13}C NMR (101 MHz, $CDCl_3$) δ 206.22 (C_q), 154.88 (C_q), 136.73 (C_q), 131.23 (CH), 130.18 (CH), 129.54 (C_q), 123.63 (C_q), 104.39 (C_q), 98.38 (CH_2), 36.44 (CH_2), 25.69 (CH_2), –0.04 (CH_3).

Synthesis of 5-ethynylindane-1-one.[27]

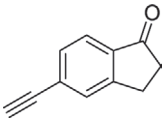

A mixture of 2,3-dihydro-5-[2-(trimethylsilyl)ethynyl] inden-1-one (40.0 g, 175 mmol, 1.0 eq.) and K_2CO_3 (12.0 g, 87.5 mmol, 0.5 eq.) in MeOH (200 mL) was stirred at RT for 2 h and monitored by TLC until full conversion was observed. The reaction mixture was concentrated and CH_2Cl_2 and water were added. The CH_2Cl_2 layer was washed with water (twice) and brine, and dried over Na_2SO_4. After filtration the mixture was concentrated under reduced pressure, and the crude product was purified by chromatography on silica gel (4:1 EtOAc/hexane) and 5-ethynylindane-1-one was isolated as a brown solid (25.0 g, 89%). ^{1}H NMR (400 MHz, $CDCl_3$) δ 7.71 (*d*, J = 7.9 Hz, 1H), 7.60 (*s*, 1H), 7.47 (*d*, J = 7.8 Hz, 1H), 3.25 (*s*, 1H), 3.13 (*t*, J = 6.0 Hz, 2H), 2.73–2.70 (*m*, 2H). ^{13}C NMR (101 MHz, $CDCl_3$) δ 206.17 (C_q), 154.91 (C_q), 137.12 (C_q), 131.39 (CH), 130.48 (CH), 128.50 (C_q), 123.75 (CH), 83.14 (C_q), 80.51 (CH), 36.43 (CH_2), 25.72 (CH_2).

Synthesis of 5-Ethenylindane-1-One (Vinylindanone):

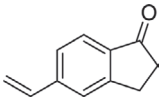

5-ethynylindane-1-one (3.7 g, 23.6 mmol, 1.0 eq.) was suspended in EtOH (100 mL) and Lindlar's catalyst (110 mg, 3 weight%) was added. The reaction flask was capped with a septum and the air was replaced with H_2 (balloon), after which the reaction mixture was stirred vigorously for 2–16 h. Importantly, to prevent over-reduction into the alkane, samples were frequently taken from the reaction mixture and, after evaporation of EtOH under reduced pressure, the conversion was determined by ^{1}H-NMR. After >90% conversion, the H_2-filled balloon was removed and the reaction mixture was concentrated under reduced pressure. The crude product was re-dissolved in CH_2Cl_2 and the catalyst was removed by filtration over Hyflo. The filtrate was concentrated under reduced pressure, giving 5-ethenylindane-1-one as a yellow solid (3.6 g, 97%). Melting point = 26 °C, melting enthalpy = 22.9 J g^{-1}. ^{1}H NMR (400 MHz, $CDCl_3$) δ 7.71 (*d*, J = 8.0 Hz, 1H), 7.48 (*s*, 1H), 7.42 (*d*, J = 8.0 Hz, 1H), 6.78 (dd, J = 17.6 Hz, J = 10.9 Hz, 1H), 5.90 (*d*, J = 17.6 Hz, 1H), 5.42 (*d*, J = 10.9 Hz, 1H), 3.13 (*t*, J = 6.0 Hz, 2H), 2.72–2.69 (*m*, 2H). ^{13}C NMR (101 MHz, $CDCl_3$) δ 206.55 (C_q), 155.84 (C_q), 143.95 (C_q), 136.67 (C_q), 136.40 (CH), 125.72 (CH), 124.33 (CH), 124.04 (CH), 117.31 (CH_2), 36.63 (CH_2), 25.87 (CH_2).

Synthesis of 5-Ethenylindane-1-One (1-Step Route):

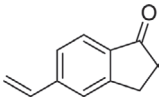

In a 10 L three necked round bottom flask 5-bromo-1-indanone (500 g, 2.37 mol, 1.0 eq.) and potassium trifluoro(vinyl)borate (381.0 g, 2.84 mol, 1.2 eq.) were dissolved in EtOH (5.0 L), and Et_3N (661 mL, 4.74 mol, 2 eq.) was added. The reaction mixture was flushed with nitrogen gas for 15 min and $Pd(dppf)Cl_2.CH_2Cl_2$ adduct (19.4 g, 23.7 mmol, 1 mol%) was added while nitrogen gas was flushed through the mixture continuously. The resulting mixture was heated to 80 °C under continuous magnetic stirring for 2–2.5 h, after which clean and complete conversion was found with GC-MS (Figure S1, Supporting Information). The reaction mixture was cooled to RT and was concentrated to a thick paste under reduced pressure. Water (2.5 L) and EtOAc (2.5 L) were added to the paste to form a two-layered system. The solids present on the interface of the layers were removed by filtration through a P3 glass frit filter. The layers were separated and the organic layer was dried over Na_2SO_4 and concentrated under reduced pressure. The obtained oil was purified by filtration through a silica plug (using four weight volumes of silica) to yield 5-ethenylindane-1-one as a yellow-orange solid in good yield (318 g, 85% yield). Melting point = 42 °C, melting enthalpy = 92.8 J g^{-1} (Figure S4, Supporting Information).

Suspension Polymerization of 5-Vinyl-1-Indanone and Divinylbenzene (2-g Scale): The aqueous phase was prepared by addition of NaCl (11 mg), polymethacrylic acid sodium salt solution (468 mg of a 10% solution in water[20]) and $CaHPO_4$ (81 mg) to water (15 mL) in a glass reactor equipped with Teflon blade stirrer. The aqueous phase was stirred for 30 min at RT. The organic phase was prepared by dissolving vinylindanone (2.0 g, 12.6 mmol) in a mixture of toluene and nitrobenzene (2.84 mL, different volume ratios) in a glass vial or beaker under gently heating. Next, 80% technical grade DVB (2.5 mol%) and a 50% benzoylperoxide blend with dicyclohexyl phthalate (61 mg, 0.13 mmol, 1.0 mol%) was added to the organic phase and stirred until a homogeneous solution was obtained. The organic phase was added to the aqueous phase in the glass reactor under continuous mechanical stirring at 330 rpm, yielding an o/w emulsion. The air was replaced by flushing with N_2 for 20 min and the stirring mixture was heated to 73 °C in an oil bath for 16 h. Afterward the suspension was allowed to cool to RT and poured over a filter (cut-off 200 μm). The residue was washed with acetone and water and dried over P_2O_5 under vacuum, resulting in polyvinylindanone (pVI, 1.5–1.9 grams, 75–95%).

Suspension Polymerization of 5-Vinyl-1-Indanone and Divinylbenzene (50-g Scale): The same procedure was followed as for the suspension polymerization on a 2 gram scale synthesis, in which the reaction time was 20 instead of 16 h. The amounts of the reagents were as follows: 242 mg NaCl, 11.7 g 10% polymethacrylic acid sodium salt solution, 2.025 g $CaHPO_4$, 375 mL water, 50.0 g vinylindanone, 64 mL toluene,

7.11 mL nitrobenzene and 1.531 g 50% benzoylperoxide blend with dicyclohexyl phthalate and 1.4 mL DVB. The yield was 91.6% (45.8 grams). The T_g of the product (pVI) was 189 °C (Figure S5, Supporting Information).

Halogenation and Kurnblum Oxidation of pVI to obtain pVI-Ox: In a glass reactor equipped with a Teflon blade stirrer, pVI beads (40.0 g, 253 mmol indanone groups) were swollen in dimethylsulfoxide (DMSO) (449 mL, 6.32 mol, 25 eq.) for 30 min under continuous stirring, after which iodine (64.2 g, 253 mmol, 1.0 eq.), aqueous 57% HI (28.9 mL, 253 mmol, 1.0 eq.) and aqueous 48% HBr (171 mL, 1.52 mol, 6.0 eq.) were added at RT. One of the outlets of the reactor was capped with a septum containing a needle, to allow escape of the formed Me_2S. The suspension was stirred for 24 h at 90 °C, after which the reaction mixture was filtered (cut-off 200 µm). The residue was washed with DMSO and water until no iodine and acid were extracted from the residue (until pH of the filtrate > 5). The filtrate was dried over P_2O_5 under vacuum, resulting in pVI-Ox (49.2 g). The T_g of the product (pVI-Ox) was not determined as it gradually decomposed >140 °C (Figure S6, Supporting Information).

Characterization of Beads by SEM: The morphology of the different beads was analyzed by scanning electron microscopy (SEM, Phenom, FEI Company, the Netherlands). Dried beads were transferred onto 12-mm diameter aluminum specimen stubs (Agar Scientific Ltd., England) using double-sided adhesive tape. Prior to analysis, the beads were coated with platinum using an ion coater under vacuum. The samples were imaged using a 5 kV electron beam.

Determination of the Size of the Beads by Light Microscopy: The diameters of the beads were measured using optical microscopy, utilizing a size calibrated Nikon eclipse TE2000-U microscope equipped with a digital camera (Nikon DS-2Mv camera and Nikon DS-U1 digital adapter, with a 4 × magnification) and the NIS-elements basic research software package. Images of the beads were taken in the dry state and for 30 arbitrary beads 3 points on the perimeter of the beads were identified to allow calculation of circular diameter by the program.[40] The average diameters and standard deviations are reported.

Thermogravimetric Analysis (TGA) of Monomer and Beads: In a platinum pan the beads were heated at a rate of 10 °C min^{-1}. The weight loss during the ramp heating (and thereby the decomposition temperature) was determined on a TAinstruments TGA Q50.

Differential Scanning Calorimetry (DSC) of Monomer and Beads: In an aluminum open pan the monomer or beads were first heated from −50 till 250 °C at a rate of 10 °C min^{-1} then cooled down to −50 °C and heated to 250 °C with rate of 10 °C min^{-1}. The heat flow was monitored. The T_g (or melting point) was determined with a TAinstruments Discovery DSC. Residual solvent evaporated during the first run and therefore the results of the second run are reported.

Solid State NMR Analysis of pVI and pVI-Ox Beads: For solid-state ^{13}C NMR measurements, pVI and pVI-Ox beads were crushed and transferred into a 3.2 mm thin-wall rotor for the magic-angle spinning (MAS) solid-state NMR experiments. The cross-polarization (CP) experiments were performed on a Bruker 400 MHz, employing a spin rate of 17 kHz, 2000 µs contact time and a recycle delay of 2s for 3072 scans. The ^{13}C direct excitation spectrum was performed using a Bruker 500 MHz spectrometer at a spin rate of 12 kHz. 30° Pulses were applied with field strength of 55 and 80 kHz SPINAL64.[41] The ^{13}C relaxation time (T_1) was measured to be 40 s with an inverse recovery and the recycle delay was set to 2*T1 (80 s). All measurements (CP and direct excitation) were conducted at 25 °C, applying 80 kHz ^1H decoupling during acquisition and MAS frequency of kHz chosen to minimize the overlap of the signal with spinning sidebands.

Nitrogen Physisorption: N_2 physisorption isotherms were measured at −196 °C using a Micromeritics TriStar 3000 and TriStar II Plus apparatus. Prior to analysis, the samples were dried under vacuum at RT for 16 h. Surface areas were determined using the Brunauer–Emmett–Teller (BET) method and the total pore volumes were derived from the amount of N_2 adsorbed at $p/p_0 = 0.995$.[42] A Barrett–Joyner–Halenda (BJH) analysis was employed to determine pore size/volume distributions of the samples with the use of a Harkins-Jura thickness curve.[43,44] Due to the shrinking of the polymeric beads with increasing pressure, and subsequent expansion with decreasing pressure, the correction of the dead volume is incorrect, as by default it assumes that the solid fraction of the sample does not change in volume with pressure. As the dead volume was determined at $p/p_0 \approx 0$ and assumed constant during the measurement, the default dead volume-corrected isotherms decreased slightly with increasing pressures, which is physically meaningless. The relative deviation is largest for materials with low surface areas (<5 $m^2\ g^{-1}$) and high materials volume fractions in the measurement tubes, such as for pVI-Ox. A correction for this deformation, that is, change in dead volume with pressure was applied to these isotherms by a linear swelling function ($V_{adjusted} = a \cdot (p/p_0) + V_{original}$), in which a represents the swelling factor relative to the material's volume at $p/p_0 \approx 0$, until $dV/d(p/p_0) > 0$ was achieved for all pressures. The S_{BET} surface areas of the pVI and pVI-Ox beads were calculated from the isotherms that were corrected for these volume changes as a function of pressure.

Urea Binding of pVI-Ox Beads under Static Conditions: The pVI-Ox beads (50 mg per glass vial, 0.16 mmol of ninhydrin groups) were incubated with urea solution (5.0 mL, 30 mM, 0.15 mmol urea) in PBS in 12 glass vials. The samples were placed in an oven at 37 °C on a rotating device or shaking water bath at 50 or 70 °C. After 1, 2, 4, 8, 16, and 24 h, two glass vials per time point were taken and the beads were allowed to settle and the supernatant was removed (see Section S7, Supporting Information). To determine the maximum binding capacity of a sorbent, the sorbent beads (50 mg per vial, 0.16 mmol of ninhydrin groups) were incubated for 24 h at 70 °C with a urea solution (5.0 mL, 50 mM, 0.25 mmol urea) in PBS in two glass vials, after which the beads were allowed to settle and the urea concentration in the supernatant was determined (see Section S6, Supporting Information).

Urea Binding of pVI-Ox Beads under Dynamic Conditions: In a glass column (for a picture see Section S9, Supporting Information) pVI-Ox sorbent beads (4.0 g) were pre-wetted with PBS (20 mL) and placed on a rotating device overnight. In an Erlenmeyer, PBS (180 mL) was heated to 37 °C and pumped with a peristaltic pump through the prewetted sorbent column (making the overall volume 200 mL) for 30 min at a flow of 25 mL min^{-1}, before returning to the Erlenmeyer (for a picture see Section S9, Supporting Information). Urea (360 mg, 6 mmol, 30 mM) was added to the Erlenmeyer and the urea concentration in the Erlenmeyer after 0, 0.5, 1, 2, 4, 6, and 8 h by removing 0.5 mL of the volume.

Supporting Information

Supporting Information is available from the Wiley Online Library or from the author.

Acknowledgements

J.A.W.J. and Y.G. contributed equally to this work. The authors would like to thank Carl C.L. Schuurmans for his help with the determination of the size of the beads and Lies A.L. Fliervoet for making Figure 3 and Dr. Eelco Ruijter (VU Amsterdam) for the valuable discussions. This research was supported by the Dutch organization for Scientific Research (NWO-TTW, project 14433) and the Dutch Kidney Foundation. M.B. gratefully acknowledges NWO for funding the NMR infrastructure (Middle Groot program, grant number 700.58.102 and Groot program, grant number 175.010.2009.002). R.D. acknowledges the European Research Council (ERC) for funding (ERC-2014-CoG 648991).

Conflict of Interest

The authors declare no conflict of interest.

Keywords

chemisorption, dialysis, ninhydrin, sorbent, urea

Received: November 18, 2019
Revised: January 9, 2020
Published online: February 17, 2020

[1] J. Luo, J. B. Fan, S. Wang, *Small* **2019**, 1904076.
[2] V. Gura, M. B. Rivara, S. Bieber, R. Munshi, N. C. Smith, L. Linke, J. Kundzins, M. Beizai, C. Ezon, L. Kessler, J. Himmelfarb, *JCI Insight* **2016**, *1*, 15.
[3] J. W. Agar, *Nephrology* **2010**, *15*, 406.
[4] A. Davenport, V. Gura, C. Ronco, M. Beizai, C. Ezon, E. Rambod, *Lancet* **2007**, *370*, 2005.
[5] H. D. Lehmann, R. Marten, C. A. Gullberg, *Artif. Organs* **1981**, *5*, 278.
[6] M. K. van Gelder, J. A. W. Jong, L. Folkertsma, Y. Guo, C. Blüchel, M. C. Verhaar, M. Odijk, C. F. van Nostrum, W. E. Hennink, K. G. F. Gerritsen, *Biomaterials* **2020**, *234*, 119735.
[7] I. D. Weiner, W. E. Mitch, J. M. Sands, *Clin. J. Am. Soc. Nephrol.* **2015**, *10* , 1444.
[8] C. S. Shinaberger, R. D. Kilpatrick, D. L. Regidor, C. J. McAllister, S. Greenland, J. D. Kopple, K. Kalantar-Zadeh, *Am. J. Kidney Dis.* **2006**, *48*, 37.
[9] M. Roberts, *Nephrology* **1998**, *4*, 275.
[10] B M. J. Blumenkrantz, A. Gordon, M Roberts, A. J. Lewin, E. A. Pecker, J. K. Moran, J. W. Coburn, M. H. Maxwell, *Artif. Organs* **1979**, *3*, 230.
[11] E. Urbanczyk, M. Sowa, W. Simka, *J. Appl. Electrochem.* **2016**, *46*, 1011.
[12] V. Wernert, O. Schaf, H. Ghobarkar, R. Denoyel, *Microporous Mesoporous Mater.* **2005**, *83*, 101.
[13] M. J. Poss, H. Blom, A. Odufu, R. Smakman, U. S. Patent 6, 861, 473 B2: **2005**.
[14] D. Deepak, *Med. Biol. Eng. Comput.* **1981**, *19*, 701.
[15] Y. C. Cheng, C. C. Fu, Y. S. Hsiao, C. C. Chien, R. S. Juang, *J. Mol. Liq.* **2018**, *252*, 203.
[16] C. Giordano, R. Esposito, P. Bello, E. Quarto, F. M. Gonzalez, *J. Dialysis* **1976**, *1*, 165.
[17] M. K. van Gelder, S. M. Mihaila, J. Jansen, M. Wester, M. C. Verhaar, J. A. Joles, D. Stamatialis, R. Masereeuw, K. G. F. Gerritsen, *Expert Rev. Med. Devices* **2018**, *15*, 323.
[18] M. N. Z. Abidin, P. S. Goh, A. F. Ismail, N. Said, M. H. D. Othman, H. Hasbullah, M. S. Abdullah, B. C. Ng, S. Kadir, F. Kamal, *Carbohydr. Polym.* **2018**, *201*, 257.
[19] R. Smakman, A. W. van Doorn, *Clin. Nephrol.* **1986**, *26*, S58.
[20] J. A. W. Jong, Y. Guo, C. Veenhoven, M. E. Moret, J. van der Zwan, A. Lucini Paioni, M. Baldus, K. C. Scheiner, R. Dalebout, M. J. van Steenbergen, M. C. Verhaar, R. Smakman, W. E. Hennink, K. G. F. Gerritsen, C. F. van Nostrum, *ACS Appl. Polym. Mater.* **2019**, *in press*, https://doi.org/10.1021/acsapm.9b00948.
[21] T. Shimizu, S. A. Fujishige, *J. Biomed. Mater. Res.* **1983**, *17*, 597.
[22] J. A. W. Jong, R. Smakman, M. E. Moret, M. C. Verhaar, W. E. Hennink, K. G. F. Gerritsen, C. F. van Nostrum, *ACS Omega* **2019**, *4*, 11928.
[23] J. A. W. Jong, M. E. Moret, M. C. Verhaar, W. E. Hennink, K. G. F. Gerritsen, C. F. van Nostrum, *ChemistrySelect* **2018**, *3*, 1224.
[24] R. Smakman, U.S. Patent 4,897,200, **1990**.
[25] A. M. Buysse, N. M. Niyaz, D. A. Demeter, Y. Zhang, M. J. Walsh, A. Kubota, R. Hunter, T. K. Trullinger, C. T. Lowe, D. Knueppel, A. Patny, N. Garizi, P. R. LePlae Jr, F. Wessels, R. Ross Jr, C. Deamicis, P. Borromeo, U.S. Patent 0213448 A1, **2014**.
[26] C. G. Bluchel, Y. Wang, K. C. Tan, U. S. Patent 0171713 A1, **2011**.
[27] R. Ortega, H. Hubner, P. Gmeiner, C. F. Masaguer, *Bioorg. Med. Chem. Lett.* **2011**, *21*, 2670.
[28] G. A. Molander, A. R. Brown, *J. Org. Chem.* **2006**, *71*, 9681.
[29] M. T. Gokmen, F. E. Du Prez, *Prog. Polym. Sci.* **2012**, *37*, 365.
[30] D. M. Van Krevelen, in *Properties of Polymers*, Elsevier, Amsterdam, **1990**, pp. 198–203.
[31] R. F. Fedors, *Polym. Eng. Sci.* **1974**, *14*, 147.
[32] H. Matsukawa, S. Yoda, Y. Okawa, K. Otake, *Polymers* **2019**, *11*, 246.
[33] N. R. Cameron, A. Barbetta, *J. Mater. Chem.* **2000**, *10*, 2466.
[34] C. M. Hanssen, in *The Three Dimensional Solubility Parameter and Solvent Diffusion Coefficient, Their Importance in Surface Coating Formulation*, Danish Technical Press, Copenhagen **1967**.
[35] W. K. Cheah, Y. L. Sim, F. Y. Yeoh, *Mater. Chem. Phys.* **2016**, *175*, 151.
[36] L. D. Wilson, C. Xue, *J. Appl. Polym. Sci.* **2013**, *128*, 667.
[37] A. Pines, M. G. Gibby, J. S. Waugh, *Chem. Phys. Lett.* **1972**, *15*, 373.
[38] R. Vanholder, T. Gryp, G. Glorieux, *Nephrol., Dial., Transplant.* **2018**, *33*, 4.
[39] H. Talke, G. E. Schubert, *Klin. Wochenschr.* **1965**, *43*, 174.
[40] C. C. L. Schuurmans, A. Abbadessa, M. A. Bengtson, G. Pletikapic, H. B. Eral, G. Koenderink, R. Masereeuw, W. E. Hennink, T. Vermonden, *Soft Matter* **2018**, *14*, 6327.
[41] B. M. Fung, A. K. Khitrin, K. Ermolaev, *J. Magn. Reson.* **2000**, *142*, 97.
[42] M. Thommes, K. Kaneko, V. A. Neimark, P. O. James, F. Rodriguez-Reinoso, J. Rouquerol, S. W. Sing Kenneth, *Pure Appl. Chem.* **2015**, *87*, 1051.
[43] E. P. Barrett, L. G. Joyner, P. P. Halenda, *J. Am. Chem. Soc.* **1951**, *73*, 373.
[44] G. Jura, W. D. Harkins, *J. Am. Chem. Soc.* **1944**, *66*, 1356.